Article

Highly Ordered "Defect-Free" Self-Assembled Hybrid Films with a Tetragonal Mesostructure

Paolo Falcaro, Stefano Costacurta, Giovanni Mattei, Heinz Amenitsch, Augusto Marcelli, Mariangela Cestelli Guidi, Massimo Piccinini, Alessandro Nucara, Luca Malfatti, Tongjit Kidchob, and Plinio Innocenzi

J. Am. Chem. Soc., **2005**, 127 (11), 3838-3846• DOI: 10.1021/ja0427956 • Publication Date (Web): 26 February 2005

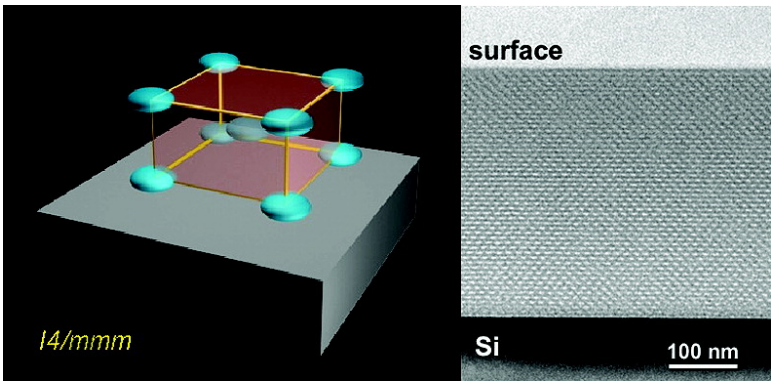

More About This Article

Additional resources and features associated with this article are available within the HTML version:

- Supporting Information
- Links to the 9 articles that cite this article, as of the time of this article download
- Access to high resolution figures
- Links to articles and content related to this article
- Copyright permission to reproduce figures and/or text from this article

View the Full Text HTML

Journal of the American Chemical Society is published by the American Chemical Society. 1155 Sixteenth Street N.W., Washington, DC 20036

J|A|C|S
ARTICLES
Published on Web 02/26/2005

Highly Ordered "Defect-Free" Self-Assembled Hybrid Films with a Tetragonal Mesostructure

Paolo Falcaro,[†] Stefano Costacurta,[†] Giovanni Mattei,[‡] Heinz Amenitsch,[§] Augusto Marcelli,[|] Mariangela Cestelli Guidi,[|] Massimo Piccinini,[|] Alessandro Nucara,[⊥] Luca Malfatti,[▽] Tongjit Kidchob,[▽] and Plinio Innocenzi*[,▽]

Contribution from the Dipartimento di Ingegneria Meccanica, Settore Materiali, Università di Padova, Via Marzolo 9, 35131 Padova, Italy, Dipartimento di Fisica "Galileo Galilei", Università di Padova, Via Marzolo 8, 35131 Padova, Italy, Institute of Biophysics and X-ray Structure Research, Austrian Academy of Sciences, Schmiedelstrasse 6, A-8042 Graz, Austria, Laboratori Nazionali di Frascati—INFN, Via E. Fermi 40, 00044 Frascati, Italy, Dipartimento di Fisica, Università di Roma "La Sapienza", P. le A. Moro 2, 00185 Roma, Italy, and Laboratorio di Scienza dei Materiali e Nanotecnologie, Nanoworld Institute, Dipartimento di Architettura e Pianificazione, Università di Sassari, Palazzo Pou Salid, Piazza Duomo 6, 07041 Alghero, Sassari, Italy

Received November 30, 2004; E-mail: plinio@uniss.it

Abstract: One-pot self-assembled hybrid films were synthesized by the cohydrolysis of methyltriethoxysilane and tetraethoxysilane and deposited via dip-coating. The films show a high "defect-free" mesophase organization that extends throughout the film thickness and for domains of a micrometer scale, as shown by scanning transmission electron microscopy. We have defined these films defect-free to describe the high degree of order that is achieved without defects in the pore organization, such as dislocations of pores or stacking faults. A novel mesophase, which is tetragonal *I4/mmm* (space group), is observed in the films. This phase evolves but retains the same symmetry throughout a wide range of temperatures of calcination. The thermal stability and the structural changes as a function of the calcination temperature have been studied by small-angle X-ray scattering, scanning transmission electron microscopy, and Fourier transform infrared spectroscopy. In situ Fourier transform infrared spectroscopy employing synchrotron radiation has been used to study the kinetics of film formation during the deposition. The experiments have shown that the slower kinetics of silica species can explain the high degree of organization of the mesostructure.

Introduction

Mesoporous materials have potential applications in microelectronics as ultralow-*k* dielectric materials and in photonics as low refractive index materials. Spin- and dip-coated hybrid materials containing methyl groups have been prepared in the past few years. Research on mesostructured silica and other inorganic oxides has grown steadily in recent years; mesoporous materials have been synthesized as powders, monoliths, and films.[1] Several studies, in particular, have focused on oxide and hybrid organic−inorganic films obtained through evaporation-induced self-assembly[2,3] (EISA), as well as on understanding mesostructure development.[4] The next step toward the fabrication of mesoporous devices is the achievement of a precise control of the properties of the material such as surface area and pore accessibility, as well as a high and reproducible mesostructural order. Novel devices based on mesostructured films are currently under development: for instance, for electrochemical and optical sensors,[5] ultralow-*k* materials for microelectronics and low refractive index materials.[6−8]

An important challenge to the chemical synthesis of organized porous films is the possibility to reach a degree of order that is extended throughout the thickness of the films and for a region of several centimeters. Up to now several authors have disclosed the potentialities of self-assembly to obtain mesostructured films

[†] Dipartimento di Ingegneria Meccanica, Settore Materiali, Università di Padova.
[‡] Dipartimento di Fisica "Galileo Galilei", Università di Padova.
[§] Austrian Academy of Sciences.
[|] Laboratori Nazionali di Frascati—INFN.
[⊥] Università di Roma "La Sapienza".
[▽] Università di Sassari.

(1) Soler-Illia, G. J. de A. A.; Sanchez C.; Lebeau B.; Patarin, J. *Chem. Rev.* **2002**, *102*, 4093.
(2) Brinker, C. J.; Lu, Y.; Sellinger, A.; Fan H. *Adv. Mater.* **1999**, *11*, 579.
(3) Grosso, D.; Boissière, C.; Smarsly, B.; Brezesinski, T.; Pinna, N.; Albouy, P. A.; Amenitsch, H.; Antonietti, M.; Sanchez, C. *Nat. Mater.* **2004**, *3*, 787.
(4) (a) Grosso, D.; Babonneau, F.; Soler-Illia, G. J. A. A.; Albouy, P. A.; Amenitsch, H. *Chem. Commun.* **2002**, 748. (b) Soler-Illia, G. J. A. A.; Crepaldi, E. L.; Grosso, D.; Durand, D.; Sanchez, C. *Chem. Commun.* **2002**, 2298. (c) Cagnol, F.; Grosso, D.; Soler-Illia, G. J. A. A.; Crepaldi, E. L.; Babonneau, F.; Amenitsch, H.; Sanchez, C. *J. Mater. Chem.* **2003**, *13*, 61.
(5) Wirnsberger, G.; Scott, B. J.; Stucky G. D. *Chem. Commun.* **2001**, 119.
(6) Jain, A.; Rogojevic, S.; Ponoth, S.; Agarwal, N.; Matthew, I.; Gill, W. N.; Persans, P.; Tomozawa, M.; Plawsky, J. L.; Simonyi, E. *Thin Solid Films* **2001**, *398*−*399*, 513.
(7) Baskaran, S.; Liu, J.; Domansky, K.; Kohler, N.; Li, X.; Coyle, C.; Fryxell, G. E.; Suntharampillai, T.; Williford, R. E. *Adv. Mater.* **2000**, *12*, 291.
(8) Balkenende, A. R.; de Theije, F. K.; Kriege, J. C. *Adv. Mater.* **2003**, *15*, 139.

 10.1021/ja0427956 CCC: $30.25

with different compositions, but only very recently the attention has been focused on the possibility of preparing ordered materials whose order can resemble that of ideal crystalline structures. It is, in fact, very important for a practical application of mesoporous films that the order is extended on a larger scale than local domains of submicrometric scale. In general, the organization is shown to be reached in terms of organized domains, similar to grains in crystalline materials.[9−10] Miyata et al.[11] have recently obtained EISA silica films with a single-crystalline mesoporous 3D-hexagonal structure maintained over a scale of centimeters. This high level of organization has been reached through epitaxial growth of a self-organized mixture of silicon alkoxide and organic templates on a rubbing-treated polyimide layer. However, the presence of an organic interlayer between the film and the substrate can undermine the mechanical and thermal stability of the film.

In other cases defects in the porous organization that can be compared to atomic dislocations in crystalline solids are observed.[16] It is important, however, to reach a full "defect-free" organization within all of the film to satisfy most of the requirements for new devices in nanotechnologies.

The mesostructural instability of this type of material, especially when exposed to the combined action of heat, pressure. and water, is another critical feature. In a previous work,[12] mesostructured silica thin films and monoliths stable up to 950 °C were synthesized using block copolymers (e.g., Pluronic F127) and performing suitable thermal post-treatments. A full removal of the silanols on the pore surface was achieved after thermal calcination at 750 °C, without significant loss of pore organization. Dehydroxylation is a fundamental step in the preparation of this material, because the presence of OH groups makes the environment hydrophilic, causing the material to adsorb large amounts of water, bonded to the pore surface, resulting in a decrease in material performance.[13]

Different strategies have been employed to synthesize mesoporous films with a hydrophobic surface, most of which have been selected keeping in mind that ultralow-*k* dielectric materials can represent a fundamental breakthrough for this new class of materials. In the majority of these methods, methyl groups have been used to form hydrophobic hybrid mesoporous films.

The preparations basically differ in the methods by which methyl groups are introduced to functionalize the surface and make it hydrophobic. Three main methods can be taken into consideration: postpreparation grafting, one-pot co-self-assembly, and vapor infiltration. Though several slight modifications have been proposed by different authors, all of the syntheses can be somehow classified within these groups. The most common approach to remove the silanols and make the material hydrophobic is to react the residual silanols in thermally calcined silica films with hexamethyldisilazane (HMDS) or trimethylchlorosilazane (TMCS) in a postpreparation treatment (grafting methods). Previously, vapor-phase reaction of HDMS has been shown to be effective in removing the silanols and therefore lowering the effective dielectric constant.[14] Other alternative routes have been proposed, such as in situ derivatization of the precursor solution with TMCS,[15] self-assembly using diblock copolymers and MTES to obtain pore isolation,[16] cohydrolysis and self-assembly of methyltriethoxysilane (MTES)−tetraethyl orthosilicate (TEOS) mixtures (one-pot EISA),[4,14,8] and MTES vapor infiltration techniques.[17]

In this work we have synthesized hybrid mesostructured films prepared by cohydrolysis and self-assembly of an optimized MTES−TEOS mixture with the purpose to reach a large order in the pore organization without "point defects". The synthesis that we report results in a high organization of the films, which appear defect-free. We have used these films to introduce a rigorous methodology, based on TEM and SAXS analysis followed by a computer simulation, to identify phases in these mesoporous films. By this approach we were able to identify a new tetragonal mesophase in the final material. We have also used in situ analytical techniques, such as SAXS and infrared spectroscopy using synchrotron radiation, to investigate and explain the high organization that we have observed in comparison to that of other mesoporous systems.

Experimental Section

See the Supporting Information.

Results and Discussion

Identification of the Mesophases. The EISA of thin films typically yields organized porous structures whose porosity lies in the 2−50 nm range (mesopores). Generally, the identification of the mesophase is not straightforward, since 1-D X-ray analysis does not allow an easy indexing of the diffraction patterns. SAXS techniques using synchrotron light are, therefore, effectively applied to achieve a better identification of the organized phases. In situ SAXS techniques have been widely used to study the mechanisms of mesophase formation in films synthesized via EISA, where phase transformation is induced by solvent evaporation.[18] In addition, a phase transformation in mesostructured films is induced by the post-deposition thermal treatment, performed to achieve the removal of the templating agent and the condensation of pore walls. This latter effect has been generally recognized by several authors;[10,19] however, a clear identification of the involved phase transitions is seldom reported.[10] This is related to the difficult interpretation of SAXS patterns and to the lack of a codified procedure to achieve phase identification in the case of mesostructured films.

We have employed GI-SAXS to record four diffraction images, corresponding to samples thermally calcined at 60, 200, 400, and 600 °C (Figure 1). The images were collected by the

(9) Klotz, M.; Albouy, P. A.; Ayral, A.; Ménager, C.; Grosso, D.; Van der Lee, A.; Cabuil, V.; Babonneau, F.; Guizard, C. *Chem. Mater.* **2000**, *12*, 1721.
(10) Besson, S.; Ricolleau, C.; Gacoin, T.; Jacquiod, C.; Boilot, J.-P. *Microporous Mesoporous Mater.* **2003**, *60*, 43.
(11) Miyata, H.; Suzuki, T.; Fukuoka, A.; Sawada, T.; Watanabe, M.; Noma, T.; Takada, K.; Mukaide, T.; Kuroda, K. *Nat. Mater.* **2004**, *3*, 651.
(12) Falcaro, P.; Grosso, D.; Amenistch, H.; Innocenzi, P. *J. Phys. Chem. B* **2004**, *108*, 10942.
(13) Maex, K.; Baklanov, M. R.; Shamiryan, D.; Iacopi, F.; Brongersma, S. H.; Yanovitskaya, Z. S. *J. Appl. Phys.* **2003**, *93*, 8793.
(14) Pai, R. A.; Humayun, R.; Schulber, T.; Sengupta, A.; Sun, J.-N.; Watkins, J. J. *Science* **2004**, *303*, 507.
(15) Yang, C.-M.; Cho, A.-T.; Pan, F.-M.; Tsai, T.-G., Chao, K.-J. *Adv. Mater.* **2001**, *13*, 1099.
(16) (a) Yu, K.; Wu, X.; Brinker, C. J.; Ripmeester, J. *Langmuir* **2003**, *19*, 7282. (b) Wu, X.; Yu, K.; Brinker, C. J.; Ripmeester, J. *Langmuir* **2003**, *19*, 7289.
(17) Tanaka, S.; Kaihara, J.; Nishiyama, N.; Oku, Y.; Egashira, Y.; Ueyama, K. *Langmuir* **2004**, *20*, 3780.
(18) Grosso, D.; Babonneau, F.; Sanchez, C.; Soler-Illia, G. J. A. A.; Crepaldi, E. L.; Albouy, P. A.; Amenitsch, H.; Balkenende, A. R.; Brunet-Bruneau, A. *J. Sol-Gel Sci. Technol.* **2003**, *26*, 561.
(19) Grosso, D.; Soler-Illia, G.; Babonneau F.; Sanchez C.; Albouy P.; Brunet-Bruneau A.; Balkenende, A. *Adv. Mater.* **2001**, *13*, 14.

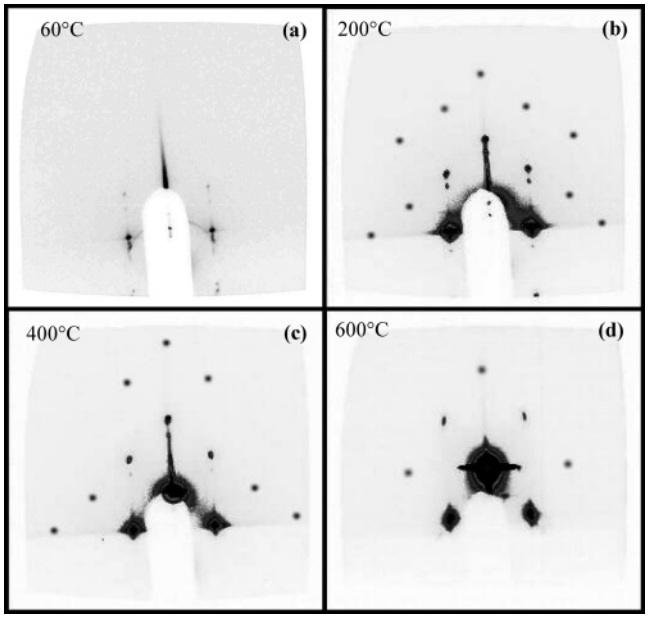

Figure 1. GI-SAXS images of the mesostructured films upon thermal calcination at (a) 60 °C, (b) 200 °C, (c) 400 °C, and (d) 600 °C.

CCD detector and processed using the FIT2D program (A. P. Hammersley/ESRF).[20] To analyze the GI-SAXS images, we have introduced some corrections by FIT2D; in particular the intensities of the images were normalized, the spatial distortion was corrected, and instrumental errors were subtracted (background noise and dark current). The intensities of the images, however, cannot be quantitatively compared because in some samples different instrumental amplifications were used to avoid signal saturation.

To identify the mesostructure, we have used the GI-SAXS image at 200 °C (Figure 1b), because the several detected diffraction spots should allow, in principle, an easier attribution of the phase with respect to the samples that exhibit a lower number of diffraction spots (Figure 1a,c,d). The spots have been obtained from images taken with different exposition times and then merged into a low saturation level diffraction image using their original positions. The reader can notice the more regular shape of the added spots.

A support to start the identification of the phase through a simulation of the diffraction spots was given by the fast Fourier transform (FFT) of the scanning mode TEM (STEM) images of the sample calcined at 200 °C (Figure 2), which suggested that the structure is body-centered tetragonal. The Fourier transform of the bright-field and dark-field, cross-section TEM image and the corresponding indexation along the [110] direction are shown in Figure 2.

To support the hypothesis of a tetragonal mesophase, we have simulated the GI-SAXS diffraction patterns of the 200 °C sample by the CMPR program (B. Toby, NIST)[21] using an *I*4/*mmm* structure (space group). The simulated patterns well reproduced the GI-SAXS spots: Figure 3 shows the enlarged GI-SAXS image of the sample calcined at 200 °C, together with the simulated image by CMPR. The GI-SAXS diffraction spots appear in the image as black bold points, while the simulated spots in agreement with the experimental GI-SAXS spots appear as red dots. Some red hollow circles indicate the simulated spots that belong to higher diffraction orders and are not observed in our GI-SAXS images. Some distortion effects are evident in the diffraction pattern: in fact some spots (marked by violet hollow squares) appear translated from their theoretical positions; we attribute this to refraction effects that may occur during scattering when the angle between the incident and scattered waves at the vacuum/sample interface is large. This phenomenon strongly influences only low-order Bragg peaks. Some extra spots (green hollow circles in Figure 3) are observable in other works (see, for example, Miyata et al.[11]), but no interpretation has been provided so far. They seem to be caused by simultaneous refraction and reflection at the film/substrate interface, followed by diffraction. These extra spots are more visible at low diffraction orders. The comparison between the simulated spectra and those experimentally obtained gives a good correspondence (Figure 3), verifying the tetragonal symmetry and allowing spot indexing. Applying the same procedure, we have also identified the mesophase in the samples upon calcination at 400 and 600 °C as tetragonal *I*4/*mmm*.

A general phenomenon observed in EISA-produced films is a phase transformation of the film mesophase during thermal shrinkage. This transformation is given by the contraction of the films in the direction orthogonal to the substrate. In several cases[4] the low-temperature mesophase, i.e., before the thermal shrinkage, has been resolved as a body-centered cubic structure, *Im*3*m*, arranged with the (110) face parallel to the substrate.[12] If the *Im*3*m* cubic cells of the as-deposited film were oriented in this way, the thermal contraction along the direction normal to the substrate would have led to an orthorhombic symmetry instead of tetragonal. On the other hand, the tetragonal structure observed here requires the starting mesophase to have an equal or a higher symmetry. In our case, therefore, it is necessary to suppose that the as-deposited mesophase has a different in-planar disposition on the substrate: the condition of coplanarity of the (001) face with the substrate implies the contraction of the *c* axis only, in accordance with the supposed phase contraction. The simulated image obtained by CMPR, generated on the basis of previous assumptions of an *I*4/*mmm* phase, was in good agreement also with the GI-SAXS image of the sample treated at 60 °C.

To support this suggested transition, we have also calculated the lattice constants of the different samples. These were calculated by means of an algorithm (eq 1),

$$S^2(a,c) = \sum_i [x_i - x_{\mathrm{th}}(a,h_i,k_i)]^2 + \sum_i [y_i - y_{\mathrm{th}}(c,l_i)]^2 = S^2(a) + S^2(c) \quad (1)$$

$$x_{\mathrm{th}} = \frac{\sqrt{(h_i^2 + k_i^2)}}{a} \qquad y_{\mathrm{th}} = \frac{l_i}{c} \quad (2)$$

implemented in Turbo Pascal programming language, which minimizes $S^2(a,c)$, which is the sum of the squares of the differences between the experimental and theoretical spots, expressed in *x*, *y* positions, as a function of the lattice parameters *a* and *c* (with *h*, *k*, *l* crystallographic indexes fixed by symmetry).

The use of this procedure is justified by the fact that the positions of the cell axes with respect to the substrate are

(20) Available at www.esrf.fr/computing/expg/subgroups/data analysis/FIT2D/index.html.
(21) http://www.ncnr.nist.gov/programs/crystallography/software/cmpr/.

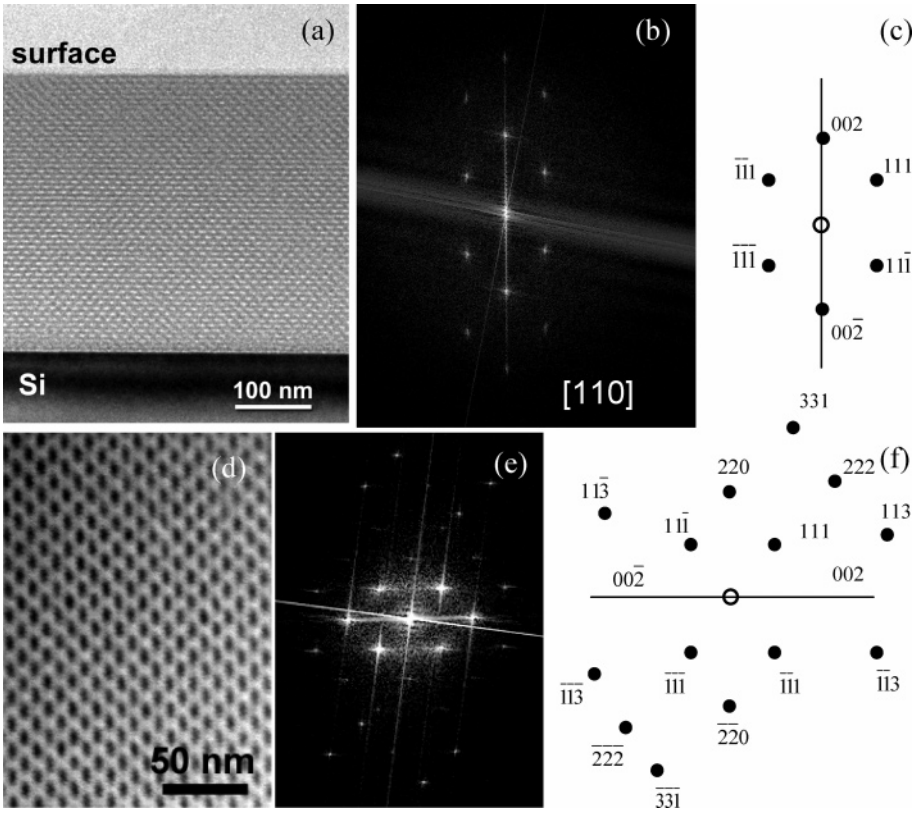

Figure 2. (a) Bright-field cross-section TEM image, (b) its Fourier transform, and (c) the correspondent indexation along the [110] direction. (d) Dark-field cross-section TEM image that is rotated 90° with respect to the image in Figure 6a, (e) its Fourier transform, and (f) the correspondent indexation along the [110] direction.

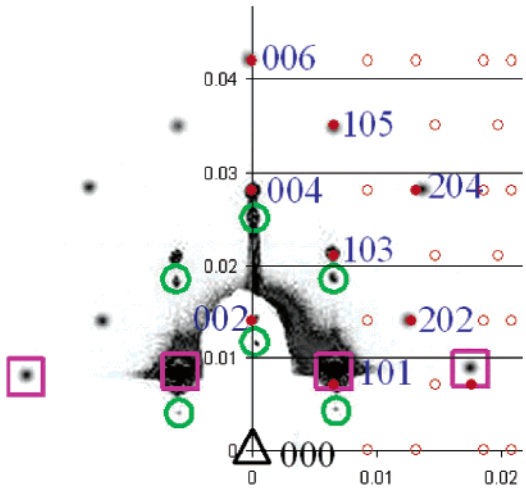

Figure 3. Comparison between the GI-SAXS image of a sample calcined at 200 °C and the computer-simulated image obtained by the CMPR program.

univocally defined. In our case only the condition of coplanarity of the (001) face with the substrate can imply the contraction of the *c* axis only: this allowed us to decouple the contributions of $a = b$ and *c* with respect to the *x* and *y* axes of the 2-D GI-SAXS patterns. From a simple error propagation it is possible to demonstrate that the percent error on *a* and *c* is the same as the error on the spot measurement in the *x*, *y* pattern.

To summarize, the GI-SAXS and TEM data show a tetragonal mesophase with *I*4/*mmm* symmetry (space group) at temperatures between 60 and 200 °C. The decrease in the lattice constant *c* that is observed with the increase of the thermal treatment can be explained by a shrinkage caused by the thermal contraction affecting the cell parameter parallel to the direction of contraction. The phase transition between body-centered tetragonal (*I*4/*mmm*) with $a < c$ to a structure having the same symmetry but with $a > c$ is illustrated in Figure 4. The tetragonal cell is oriented with the (001) plane parallel to the substrate (*c* axis normal to the substrate); after the thermal treatment, a decrease of the cell parameters takes place, markedly in the [001] direction perpendicular to the substrate, causing the shrinkage of the structure along this direction. This effect has been previously reported in the case of silica mesostructured films obtained with TEOS as the single silica source[4,9,22] and can be extended to the MTES hybrid films produced here. The difference in the composition of the mesophases in these two cases implies a fundamental difference in symmetry and in the thermal evolution. Thus, the presence of the methyl groups seems to play a fundamental role during the self-assembly process, modifying the packing of micelles inside the as-deposited film.

The decrease of the cell parameters with increasing calcination temperatures (Figure 5) is in accordance with the phase transition model suggested here: the *a* and *b* axes do not vary significantly within the experimental error, while the *c* axis shows a decrease from 23.4 nm at 60 °C to 14.3 nm at 600 °C, corresponding to a shrinkage of 39%. In a previous work[12] mesostructured silica films were obtained using TEOS as the silica precursor and Pluronics F127 as the templating agent, and the deposition was performed in the same experimental conditions as those

(22) Doshi, D. A.; Gibaud, A.; Goletto, V.; Lu, M.; Gerung, H.; Ocko, B.; Han, S. M.; Brinker, C. J. *J. Am. Chem. Soc.* **2003**, *125*, 11646.

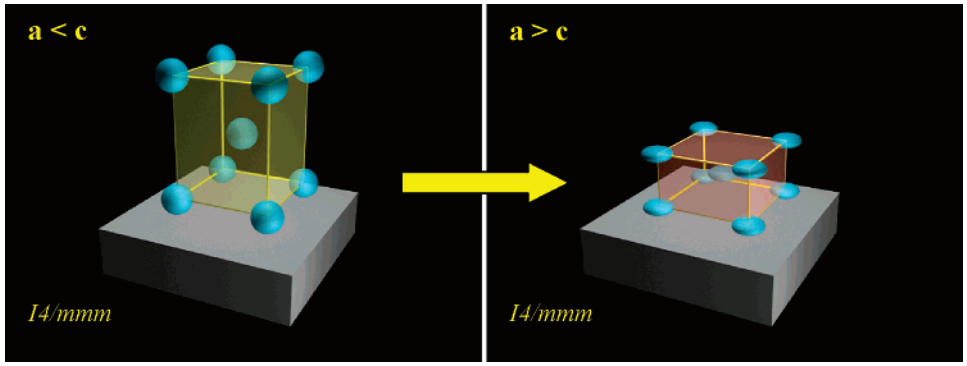

Figure 4. Representative pictures of the contraction of *c* for an *I*4/*mmm* mesostructure from 60 to 600 °C. *c* axis normal to the substrate.

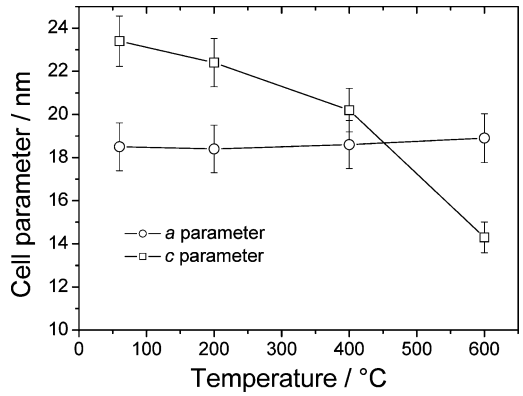

Figure 5. Variation of *a* (circles) and *c* (squares) cell parameters as a function of the thermal treatment. The lines are a guide for the eyes.

employed in this work (RH, speed rate, thermal treatment). The calculated percent contraction of the lattice parameter perpendicular to the substrate was 34%.

Shrinkage following thermal treatment in MTES-derived mesostructured films has been observed previously by other authors, without, however, identification of a similar phase.[23]

The high degree of order reached in the MTES-derived self-assembled mesostructured films can be directly observed by TEM images. A bright-field cross-section TEM image is shown in Figure 6a. The silicon substrate appears as a dark layer in the bottom part of the figure; the thickness of the film is 370 nm (±5 nm). The film appears highly ordered with elliptical pores, due to the thermally induced shrinkage along the direction normal to the substrate. In the dark-field cross-section STEM images (Figure 6b) of a sample treated at 350 °C, the structural order and the elliptical shape (enlargement in Figure 6c) are clearly observed. The pore dimensions measured from the TEM images are 8.8 nm ($\sigma = \pm 0.9$ nm) along the major axis, parallel to the surface, and 4.8 nm ($\sigma = \pm 0.5$ nm) along the minor axis, perpendicular to the substrate, with a 1.8 nm ($\sigma = \pm 0.3$ nm) ratio between the longer and shorter axes.

Kinetics of Film Formation during EISA. The formation of an organized mesophase results from the balance of different competitive kinetic processes: inorganic polycondensation and phase separation or organization of the template.[24] In silica systems at low pH (~2), the condensation rates are slow enough to allow the formation of ordered phases during self-assembly. Speeding up of the silica reactivity gives, in general, a lower degree of organization, in accordance with the ideal order for self-assembly of the kinetic constants involved in the process:[25]

$$k_{\text{inter}} > k_{\text{org}} > k_{\text{inorg}} \qquad (3)$$

While from a theoretical point of view the relationship between kinetic processes and order is well assessed, there is a lack of experimental evidence in self-assembled films to correlate the kinetics of inorganic polycondensation with micelle organization into a final organized phase. The difficulty in performing a reliable set of experiments is, in fact, a serious limitation. In situ experiments were done by SAXS; however, they give information only on phase formation, but not on polycondensation kinetics during EISA. An interesting possibility is to apply vibrational spectroscopies, such as FTIR "in situ" during EISA. An example of this kind of study has been reported by Doshi et al.,[22] but the results are not very informative because the scale of time employed is too big to allow an investigation of film formation. We have used infrared synchrotron radiation to perform "real time" in situ analysis during EISA. The main advantage of the experimental configuration that we have used is that we can record the spectra in transmission, with a good signal-noise ratio, even on a short time scale with the possibility to focus the IR beam in a smaller sample region. We have also coupled this analysis with in situ SAXS experiments in transmission during dip-coating. The in situ conditions of analysis between IR and SAXS experiments are different because we measured EISA in cast (IR) or dip-coated (SAXS) films, but since we have a correlated set of the same samples, a comparison of the trends was highly informative.

As previously pointed out and observed by other researchers, the MTES−TEOS system gives a better and easier organization during EISA with respect to other systems such as silica, titania[3], zirconia, or hybrid compositions.[26] We have also observed during our experiments that self-assembly with MTES−TEOS is highly reproducible and less sensitive to variations in deposition parameters such as relative humidity or withdrawal speed. Figure 7a shows the FTIR absorption transmission spectra recorded in situ during film formation in an MTES−TEOS

(23) De Theije, F. K.; Balkenende, A. R.; Verheijen, M. A.; Baklanov, M. R.; Mogilnikov, K. P.; Furukawa, Y. *J. Phys. Chem. B* **2003**, *107*, 4280.
(24) Soler-Illia, G. J. de A. A.; Crepaldi, E. L.; Grosso, D.; Sanchez, C.; *Curr. Opin. Colloid Interface Sci.* **2003**, *8*, 109.
(25) Huo, Q.; Margolese, D. I.; Ciesla, U.; Demuth, D. G.; Feng, P.; Gier, T. E.; Sieger, P.; Firouzi, A.; Chmelka, B. F.; Schüth, F.; Stucky, G. D. *Chem. Mater.* **1994**, *6*, 1176.
(26) Grosso, D.; Boissière, C.; Smarsly, B.; Brezesinski, T.; Pinna, N.; Albouy, P. A.; Amenitsch, H.; Antonietti, M.; Sanchez, C. *Nat. Mater.* **2004**, *3*, 787.

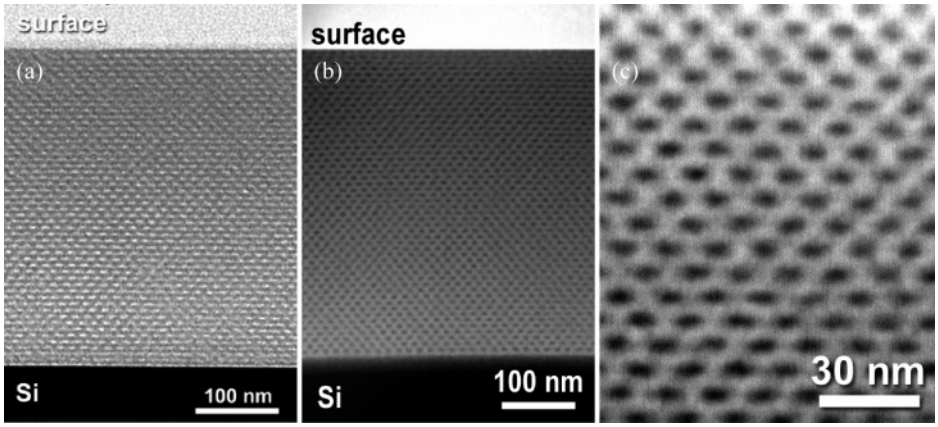

Figure 6. (a) Bright-field cross-section TEM image of a sample treated at 350 °C. (b) Dark-field cross-section TEM images in scanning mode (STEM) of a sample treated at 350 °C. (c) Enlargement of an area of the mesostructured film.

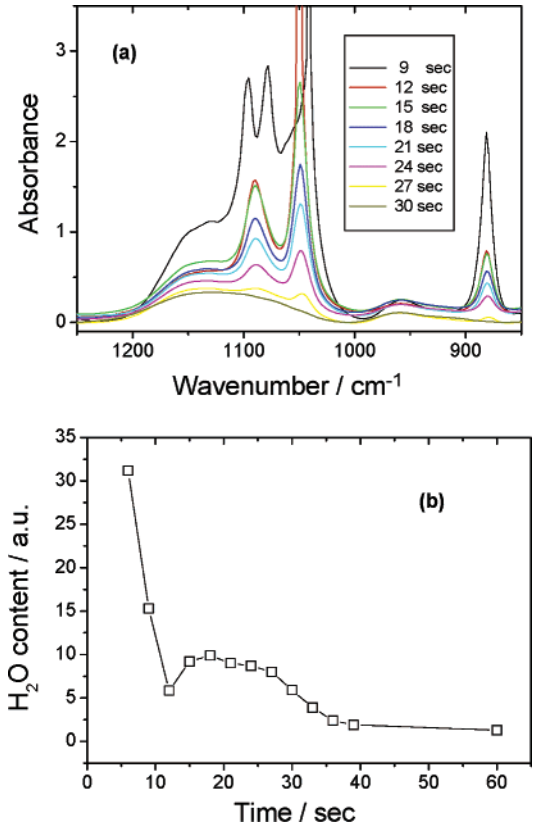

Figure 7. (a) FTIR absorption transmission spectra recorded in situ during film formation in an MTES−TEOS system without surfactant. (b) Variation in the water content in the films measured from the band at 1640 cm^{-1}. The lines are a guide for the eyes.

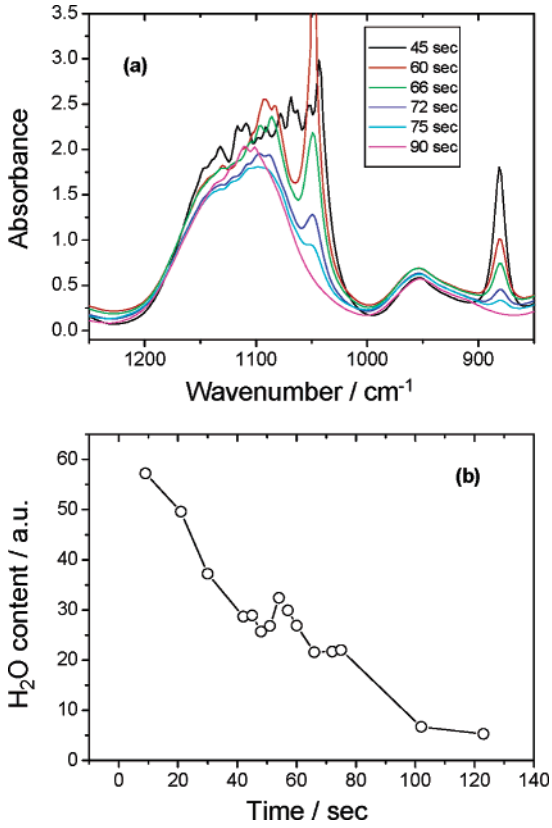

Figure 8. (a) FTIR absorption transmission spectra recorded in situ during film formation in an MTES−TEOS−F127 system during EISA. (b) Variation in the water content in the films measured from the band at 1640 cm^{-1}. The lines are a guide for the eyes.

system without surfactant. The spectrum 9 s after the deposition is still dominated by the strong signature of ethanol (883, 1044, and 1095 cm^{-1}).[30] After 15 s a significant evaporation of ethanol is observed, and the hydrolysis and condensation reactions between unreacted $SiOC_2H_5$ groups give rise to the formation of the hybrid network, as suggested by the decrease in intensity of the bands at 1096 cm^{-1} (ν_{as}(C−O) in TEOS and MTES) and 1048 cm^{-1} (ν_s(C−O) in TEOS and MTES).[27] The polycondensation reactions go to completion around 30 s after the deposition.

The decrease of the water content in the films during the deposition process is shown in Figure 7b; the variation in H_2O is measured from the area of the 1640 cm^{-1} vibrational mode. There is a very fast decrease in the water content in the first 12 s, during which H_2O is evaporating with ethanol. After this initial stage, a slight increase in correspondence with the release of water during the reactions of polycondensation is observed. On the other hand, the kinetics of polycondensation is much slower in the presence of the surfactant (Figure 8a). During EISA of the MTES−TEOS−F127 film the polycondensation stops after around 90 s, which means that, in the presence of a triblock copolymer surfactant such as the Pluronic F127, the reactions are significantly slower in comparison to a "classic"

(27) Matos, M. C.; Ilharco, L. M.; Almeida, R. M. *J. Non-Cryst. Solids* **1992**, *147*, *148*, 232.

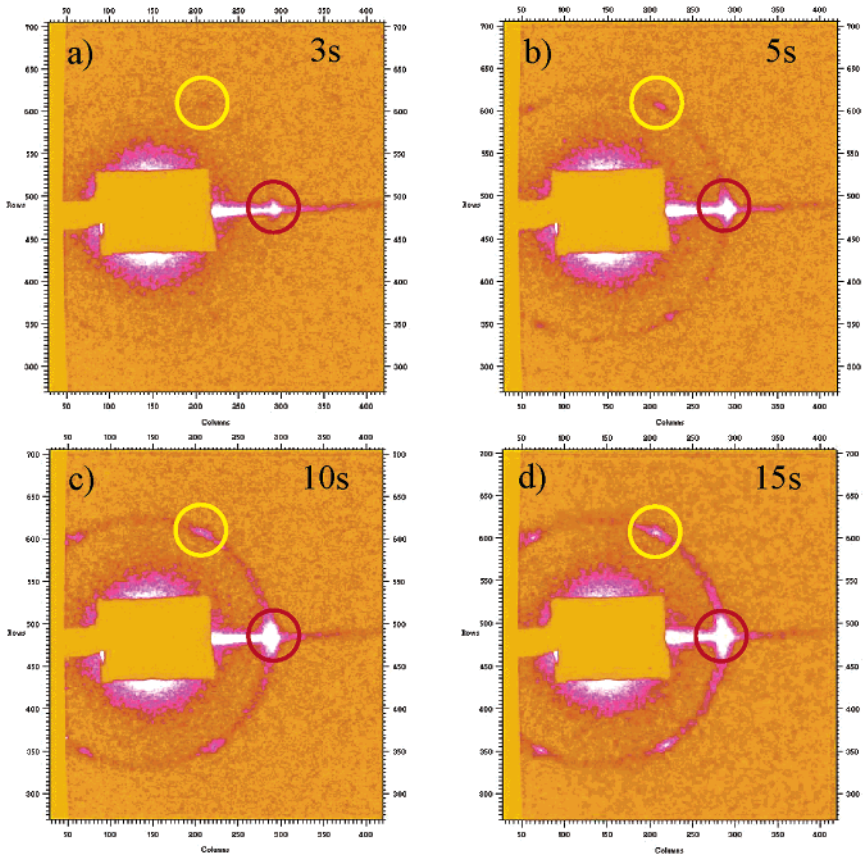

Figure 9. SAXS images taken in real time during the dip-coating of an MTES−TEOS−F127 film. Pixel scales are shown, giving to the reader the possibility to check the evolution of every single spot.

sol−gel reaction (the two solutions that we have compared are exactly the same with the exception of F127). In this case, too, we observe the same increase of water content after the first stage of fast evaporation (Figure 8b). This effect is quite important to consider to understand the details of EISA in films.

On the other hand, the SAXS images reveal that self-assembly in MTES−TEOS−F127 systems is comparatively much faster than in only TEOS−F127 solutions. Figure 9 shows the SAXS transmission images taken in situ in real time during EISA during dip-coating of films from MTES−TEOS−F127 sols. The organization of the micelles becomes faster, as a consequence of the lower kinetics of polycondensation of silica species. Only 3 s after the deposition, the diffraction spots related to the organized phase appear. This means that a fast organization takes place, much faster than in TEOS−F127 when in the same conditions up to 10−20 s can be necessary to observe the first diffraction spots (not shown in the figures).

The presence of methyl groups in the silica sol has an important role to help self-organization, in that they affect the micelle/silica interface and the kinetics of the reactions of the species involved in EISA. The strong interactions between silica and PEO blocks are reduced by the presence of CH_3 in the silica oligomers, while at the same time k_{inorg} also becomes smaller, allowing a very high organization to be reached. In these conditions, the organization of the micelles is not hindered by a more condensed inorganic network, and a faster organization is observed.

Thermally Induced Structural Changes Studied by FTIR. The influence of methyl groups, within the mesoporous films, on water absorption at different calcination temperatures was studied by FTIR spectroscopy. FTIR absorption spectra, collected in air, of films treated at 60, 200, 400, and 600 °C are shown in Figure 10. The presence of methyl groups is revealed by the absorption peaks at 1276 cm^{-1}, due to CH_3 deformation, and 2977 cm^{-1}, due to stretching in CH_3. The intensity of these bands decreases at higher thermal calcination temperatures, indicating a removal of methyl groups from the mesostructure; at 600°C only approximately 20% of the methyl groups remain in the films. The calcination of the films is accompanied by the usual decrease in intensity of the Si−OH stretching band around 950 cm^{-1} and the shift to lower wavenumbers of the Si−O−Si antisymmetric stretching mode around 1070 cm^{-1}, indicating strengthening of the silica network due to poly-

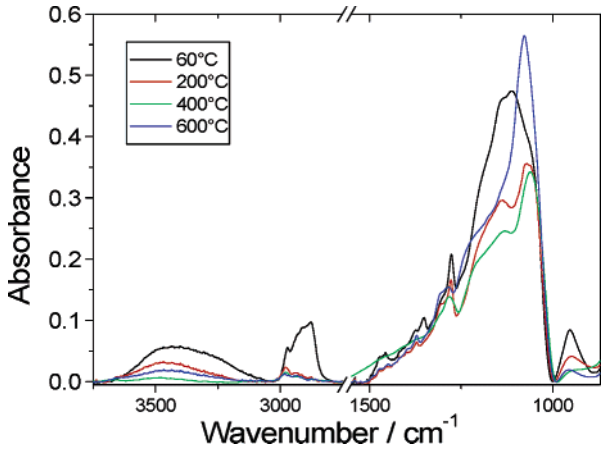

Figure 10. FTIR absorption spectra, collected in air, of films treated at 60, 200, 400, and 600 °C.

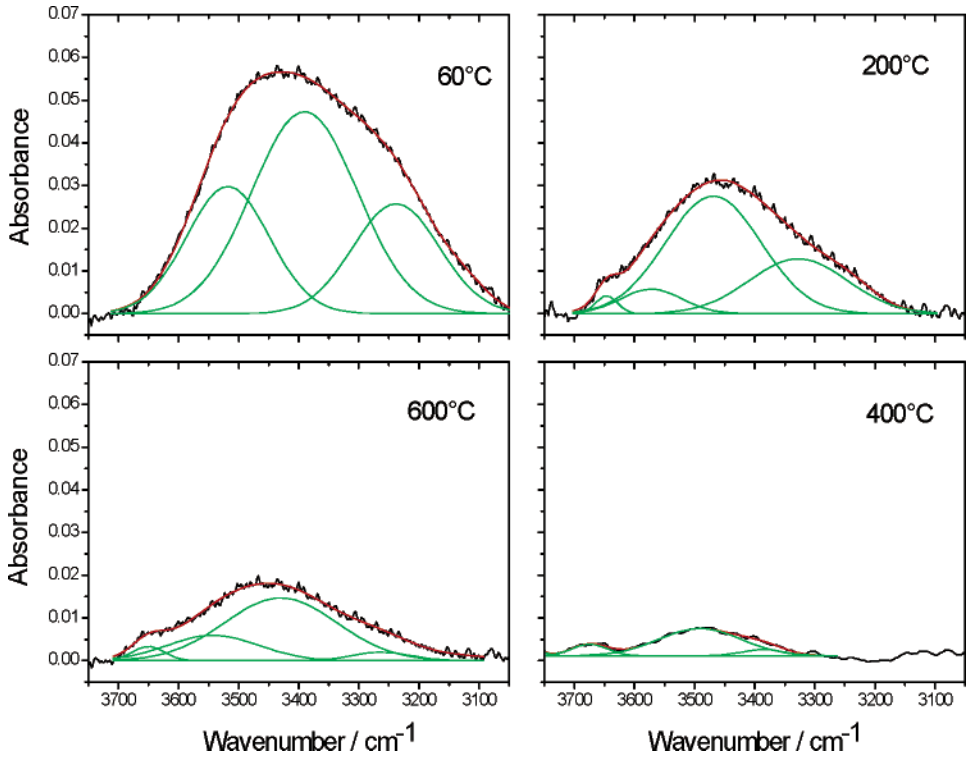

Figure 11. Deconvolution of the FTIR spectra in the range ~3000−3800 cm^{-1} for films treated at 60, 200, 400, and 600 °C.

condensation.[28] This band appears, however, composed of several overlapped bands and is generally very difficult to deconvolute.[29] In the present case a clear attribution is more complicated by the overlapping with the absorption bands in the 1050−1175 cm^{-1} interval, which are the most intense modes observed in a pure Pluronic F127 infrared spectrum[30] (C−O−C stretching (1110 cm^{-1}), C−C stretching (1150 cm^{-1}), and CH_2 rocking (1160 cm^{-1})). However, the presence of a weak and broad absorption band around 600 cm^{-1} (not shown in the figures), which is assigned to vibrations of four-membered rings within the ring plane (Si−O stretching vibrations coupled with O−Si−O and Si−O−Si bending vibrations),[31] coupled with the detection of the overlapped peak around 1135 cm^{-1}, is a good indication that 4-fold cyclic species are present in the silica framework. We suppose, in fact, that the vibrational mode at 1135 cm^{-1} is in great part due to antisymmetric stretching (Si−O−Si) in strained 4-fold siloxane rings[32] because Pluronic is nearly completely removed upon thermal calcination at 400 °C, as given by the C−H stretching bands in the 2700−3000 cm^{-1} region, but this band still remains quite intense. The formation of 4-fold rings in gels prepared in acidic conditions from MTES is well documented both for powders[33] and for films[34] and has been also observed in silica mesostructured films prepared from CTAB[29] and block copolymers.[12]

The thermal calcination of the films causes a change in the amount of methyl groups present in the mesopores while inducing thermal dehydroxylation. These two processes are simultaneous and affect the hydrophobicity of the system and, hence, the ability to absorb water. To evaluate how the thermal calcination is affecting this process, we have performed a deconvolution of the FTIR spectra in the range ~3000−3800 cm^{-1} (Figure 11). To deconvolute the FTIR spectrum of the 60 °C sample, we have selected three components, one component at the highest wavenumber assigned to terminal silanols (this band is supposed to be formed by two overlapped vibrational modes due to pairs of silanols that in this case we do not resolve), one component (~3350 cm^{-1}) due to hydrogen-bonded silanols in chains that contain more than one pair of mutually H-bonded OH groups, and a third (~3250 cm^{-1}) attributed to the first overtone of the 1640 cm^{-1} bending mode of molecular water,[35] $2\nu_b(H_2O)$. We have done some simplifications, because we have used one component for the possible two types of terminal silanol modes and because also we have used one Gaussian curve to fit the contribution from partially overlapped components due to OH stretching of silanols in chains (around 3500 cm^{-1}) and the antisymmetric stretching of molecular water bound to silica and the symmetric stretching of free or H-bonded molecular water within a silica network (~3450 cm^{-1}). In the fit of the samples calcined at higher temperatures (200, 400, and 600 °C) we have introduced another component due to the isolated silanols that are formed during dehydroxylation (~3650 cm^{-1}).

The deconvolution shows that there is a decrease in intensity of all the components after calcination at 200 °C and the dehydroxylation is practically complete at 400 °C, because only weak traces of terminal and isolated silanols are observed, without residual water. If the sample is treated at higher

(28) Innocenzi, P. *J. Non-Cryst. Solids* **2003**, *316*, 309.
(29) Innocenzi, P.; Falcaro, P.; Grosso, D.; Babonneau, F. *J. Phys. Chem. B* **2003**, *107*, 4711.
(30) Su, Y.-L.; Wang, J.; Liu, H.-Z. *Macromolecules* **2002**, *35*, 6426.
(31) Yoshino, H.; Kamiya, K.; Nasu, H. *J. Non-Cryst. Solids* **1990**, *126*, 68.
(32) Fidalgo, A.; Ilharco, L. M. *J. Non-Cryst. Solids* **2001**, *283*, 144.
(33) Kamiya, K.; Yoko, T.; Tanaka, K.; Takeuchi, M. *J. Non-Cryst. Solids* **1990**, *121*, 182.
(34) Gallardo, J.; Duran, A.; Di Martino, D.; Almeida, R. M. *J. Non-Cryst. Solids* **2002**, *298*, 219.
(35) Davis, K. M.; Tomozawa, M. *J. Non-Cryst. Solids* **1996**, *201*, 177.

temperatures, new silanols are formed and a small amount of water is absorbed (600 °C).

This process can be explained with the presence of the surfactant and methyl groups. At 60 °C the pores are filled with the block copolymer whose hydrophilic chains are able to absorb and retain water; at the same time the pore walls are covered with hydrophilic silanols. In these conditions, the hydrophobicity of the methyl groups is largely shadowed. When the surfactant is completely removed and thermal calcination is practically terminated, with the reaction of silanols the pores are covered only by methyl groups and the absorption of water is finally inhibited (400 °C). At 600 °C the methyl groups, in the presence of water, can form silanols through the reaction[36]

$$SiCH_3 + H_2O \rightarrow SiOH + CH_4 \quad (4)$$

and silica bonds can be broken by water to give the new silanol species that are observed in the FTIR spectra (Figures 10 and 11).

The curve from the fitting that is assigned to $2\nu_b(H_2O)$ was used to qualitatively investigate the change in water absorption during thermal calcination (Figure 12). In addiction, the data obtained from the $\nu_b(H_2O)$ at 1640 cm^{-1}, which is difficult to evaluate because of the instrumental noise in this wavenumber range, are well in agreement with those calculated from the deconvolution, supporting the choice done for the fit.

Conclusions

The use of MTES in the synthesis of mesostructured self-assembled silica films results in a simple and efficient way to obtain highly ordered hybrid films that we have defined as defect-free on a micrometric scale. As pointed out by structural analysis, the one-pot strategy with MTES produces, in fact, films with periodic porosity (a new tetragonal *I*4/*mmm* mesophase) which is well ordered throughout the whole thickness of the film. The approach that we have developed based on the combination of STEM, SAXS, and computer simulation has been shown to be a very effective tool for phase identification of mesoporous films.

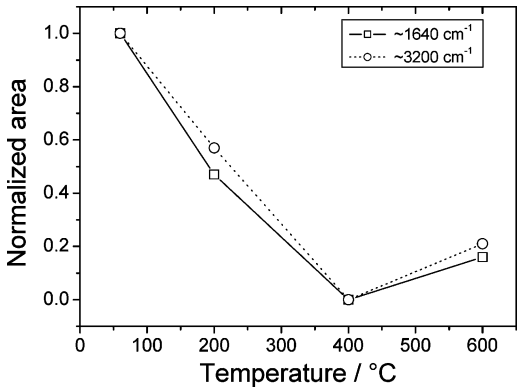

Figure 12. Area variation of peaks attributed to $\nu_b(H_2O)$ at 1640 cm^{-1} (hollow squares) and $2\nu_b(H_2O)$ at 3200 cm^{-1} (hollow circles) as a function of film thermal treatment. The lines are a guide for the eyes.

Thermal calcination of as-deposited films induces a contraction in the tetragonal *I*4/*mmm* cell parameters. FTIR analysis reveals that at 400 °C the silica films obtained using MTES are completely hydrophobic.

The kinetics of polycondensation of the hybrid silica structure is highly slowed in the presence of the surfactant, as shown by the FTIR in situ studies. This explains the high ability of self-assembly of MTES−TEOS systems.

Acknowledgment. FIRB Italian projects are acknowledged for financial support (FIRB Contract No. RBNE01P4JF). Professor Roberto Paroni (University of Sassari) and Nathan P. Mellott (University of Padova) are gratefully acknowledged for helpful discussions.

Supporting Information Available: Experimental details (PDF). This material is available free of charge via the Internet at http://pubs.acs.org.

JA0427956

(36) Sugahara, S.; Kadoya, T.; Usami, K.-I.; Hattori, T.; Matsumura, M. *J. Electrochem. Soc.* **2001**, *148*, F120.